Published in final edited form as:
Matrix Biol. 2014 April ; 35: 223–231. doi:10.1016/j.matbio.2013.12.004.

Biglycan modulates angiogenesis and bone formation during fracture healing

Agnes D. Berendsen[a], **Emily L. Pinnow**[a], **Azusa Maeda**[a], **Aaron C. Brown**[a], **Nancy McCartney-Francis**[a], **Vardit Kram**[a], **Rick T. Owens**[b], **Pamela G. Robey**[a], **Kenn Holmbeck**[a], **Luis F. de Castro**[a], **Tina M. Kilts**[a], and **Marian F. Young**[a,*]

[a] Craniofacial and Skeletal Diseases Branch, NIDCR, NIH, Bethesda, MD 20892, USA

[b] LifeCell Corporation, Branchburg, NJ 08876, USA

Abstract

Matrix proteoglycans such as biglycan (Bgn) dominate skeletal tissue and yet its exact role in regulating bone function is still unclear. In this paper we describe the potential role of (Bgn) in the fracture healing process. We hypothesized that Bgn could regulate fracture healing because of previous work showing that it can affect normal bone formation. To test this hypothesis, we created fractures in femurs of 6-week-old male wild type (WT or Bgn+/*0*) and Bgn-deficient (Bgn-KO or Bgn−/*0*) mice using a custom-made standardized fracture device, and analyzed the process of healing over time. The formation of a callus around the fracture site was observed at both 7 and 14 days post-fracture in WT and Bgn-deficient mice and immunohistochemistry revealed that Bgn was highly expressed in the fracture callus of WT mice, localizing within woven bone and cartilage. Micro-computed tomography (μCT) analysis of the region surrounding the fracture line showed that the *Bgn*-deficient mice had a smaller callus than WT mice. Histology of the same region also showed the presence of less cartilage and woven bone in the *Bgn*-deficient mice compared to WT mice. Picrosirius red staining of the callus visualized under polarized light showed that there was less fibrillar collagen in the Bgn-deficient mice, a finding confirmed by immunohistochemistry using antibodies to type I collagen. Interestingly, real time RT-PCR of the callus at 7 days post-fracture showed a significant decrease in relative vascular endothelial growth factor A (VEGF) gene expression by Bgn-deficient mice as compared to WT. Moreover, VEGF was shown to bind directly to Bgn through a solid-phase binding assay. The inability of Bgn to directly enhance VEGF-induced signaling suggests that Bgn has a unique role in regulating vessel formation, potentially related to VEGF storage or stabilization in the matrix. Taken together, these results suggest that Bgn has a regulatory role in the process of bone formation during fracture healing, and further, that reduced angiogenesis could be the molecular basis.

Keywords

Biglycan; Fracture healing; Angiogenesis; Callus; Mineralization

* Corresponding author at: Building 30 Room 225, NIDCR, NIH, Bethesda, MD 20892, USA. Fax: +1 301 402 0824. myoung@dir.nidcr.nih.gov (M.F. Young)..

Ethical statement
The authors have nothing to declare.

1. Introduction

Bone fracture repair involves a complex sequence of physiological events, each of which has important roles in the ultimate healing process (Einhorn, 1998; Manigrasso and O'Connor, 2004). Immediately after fracture, a hematoma forms around the traumatized site that is then infiltrated with immune cells. Fibrous tissue subsequently forms around the injured site and develops into a soft callus containing newly formed cartilage. Blood vessel ingrowth is then initiated adjacent to the cartilage allowing the transfer of nutrients for the newly forming woven bone in a structure referred to as a hard callus. The callus has an important role in providing structure and support to the healing bone. The final phase of fracture healing is a remodeling (removal and repair) of the temporary bone, leading to its replacement by a cortical bone and intramedullary bone. If healed properly, the remodeled bone will resemble the original bone prior to the fracture in both structure and strength.

Fracture healing requires a fine interplay between numerous cell types and the unique extra-cellular matrices (ECM) that they elaborate. Besides being the infrastructure in which cells reside, the ECM serves as a reservoir for many cytokines and growth factors whose bioavailability is strictly regulated. For example, bone morphogenic protein 2 (BMP2) stored in the ECM is released from the fracture site and helps recruit osteoprogenitor cells from the periosteum in the initial stages of fracture repair (Barnes et al., 1999). Moreover, the ECM integrity plays a pivotal role in bone toughness, both before and after fracture [e.g., the ability to dissipate energy and resist crack propagation during the actual break]. Type I collagen, which comprises 90% of the organic matrix, is the primary determinant of bone toughness and is critical for overall fracture resistance (Nyman and Makowski, 2012). Disruption of collagen integrity due to increased amounts of non-enzymatic collagen crosslinking reduces bone strength and post-yield energy dissipation, enabling the formation and easy propagation of more microdamage in the ECM. Noncollagenous proteins (NCPs) also contribute to the fracture resistance of bone as they can bridge neighboring mineralized collagen fibrils (Nyman and Makowski, 2012). The precise nature of the numerous collagen and noncollagenous proteins found in bone is quite complex and includes multiple families including fibrillar and non-fibrillar collagens, the SIBLINGs (small integrin-binding ligand N-linked glyco-proteins), matricellular proteins, large modular proteoglycans as well as small proteoglycans known as SLRPs (small leucine-rich proteogly-cans) (Iozzo et al., 2011).

Biglycan (Bgn) is a member of the SLRP family that is highly abundant in bone (Fisher et al., 1983) and its surrounding musculoskeletal tissues (Bianco et al., 1990). Bgn-deficient mice have a reduced growth rate and decreased bone mass due to lower levels of bone formation (Xu et al., 1998). Bgn appears to regulate bone cell function by directly binding to BMP2 and regulating its ability to stimulate downstream signaling and ultimately bone cell differentiation (Chen et al., 2004). For many years, BMP2 has been the focus of intense investigation because of its ability to induce new bone formation. Interestingly, mice unable to make BMP2 in their limbs have earlier and more severe spontaneous fractures as they age, providing additional proof of the essential role of BMP2 in fracture healing (Tsuji et al., 2006). Considering that Bgn regulates BMP2 activity and, further, that BMP2 regulates fracture healing, we hypothesized that the absence of Bgn could affect the fracture healing

process. In the current study, we present new data showing that Bgn has a potential role in fracture healing and provide evidence that it binds directly to VEGF, an important factor in vessel formation. We propose that this binding could in some way modulate vessel formation which is diminished in the callus of the healing Bgn-deficient mice. Taken together we show novel roles for Bgn in regulating angio-genesis and new bone formation during fracture healing.

2. Results

2.1. Bone healing in WT and Bgn-deficient mice assessed by X-ray and μCT

Fractures were created in femurs using a standardized fracture device (Fig. 1) with WT and Bgn-deficient mice male mice at 6 weeks of age, and the healing process was followed weekly for a period of 4 weeks. Immediately after the induced fracture, the mice were X-rayed and during this procedure, we noticed that the bones of the *Bgn*-deficient mice fractured more easily than the bones of WT mice. Specifically, when the same size weight was applied to create the fractures we consistently found twice as many bones broken in the *Bgn*-deficient mice compared to WT. Subsequently, we used only mice with comparable oblique bone fractures for further study. As has been noted previously in normal mice (Morgan et al., 2009), the bones from WT mice formed a large callus within 2 weeks after fracture (Fig. 2). Fractured bones from *Bgn*-deficient mice formed a smaller callus compared to WT mice and, further, appeared to have delayed healing (Fig. 2). Additional analysis by μCT confirmed this finding (Fig. 3A), and quantification of the callus area at 14 days post-fracture revealed that the cross sectional area (CSA) of the callus was significantly lower in the *Bgn*-KO mice compared to WT mice (Fig. 3B). At 7 days post-fracture the expression of alkaline phosphatase (*Alp*), a marker of bone differentiation was significantly decreased in the callus of Bgndeficient mice compared to WT mice (Fig. S1).

2.2. Bgn and aggrecan (acan) expression in the bone callus

To identify the location of Bgn expression in the fracture healing process, and further, to learn more about how Bgn could affect the callus, WT and *Bgn*-deficient mice were analyzed 14 days post-fracture by histology and immunohistochemistry. These experiments confirmed our notion that *Bgn*-deficient mice form smaller calluses compared to WT mice (Fig. 4A), and further, that Bgn is well positioned to play a role in the repair process, being localized in the woven bone forming around the cartilage (Fig. 4B, arrowheads). As predicted, Bgn staining (Fig. 4B) and mRNA expression (Fig. 4C) are negligible in the *Bgn*-KO tissue. Interestingly, the expression of the related SLRP, decorin (Dcn), was also found in the callus and appeared to be elevated in the Bgn-deficient bones (Fig. S2). The cartilage formation in the callus also appeared to be reduced in the *Bgn*-deficient mice judged by H&E staining, as well as by the reduced expression of the proteoglycan Acan (Fig. 4D). The molecular foundation for the reduction of Acan protein appeared to arise from a corresponding decrease in Acan mRNA levels in *Bgn*-deficient callus relative to WT callus 7 days post-fracture (Fig. 4E).

2.3. Collagen staining in the healing callus

Considering the importance of collagen in bone, and the fact that Bgn can regulate collagen fibril formation (Ameye and Young, 2002), we next compared the nature of collagen fibrils in WT and *Bgn*-KO-fractured bones using picrosirius red (a specific collagen staining) and immunohistochemistry using antibodies specific for type I collagen (Col1a1). As predicted from the reduced size of the callus of the mutant mice the amount of Col1a1 covered area was reduced in the Bgn-deficient bone both in the newly formed bone around the callus as well as in the cortical bone itself (Fig. 5A, B).

2.4. Relationship of Bgn to vascularization in healing bone

Close inspection of the healing callus by H&E staining indicated that in the *Bgn*-KO the newly formed bone contained less vascularization (Fig. 6A, arrowheads, bottom panel). In order to estimate the amount of blood vessel formation in the WT compared to *Bgn*-deficient callus we next stained the tissue sections with an HRP-conjugated lectin that shows specific affinity for the vascular endothelial cells glycocalix. This latter analysis showed that the vessels invading the bone (red arrowheads) adjacent to the cartilage (black arrowheads) were less abundant in the *Bgn*-deficient callus compared to WT controls (Fig. 6B) and when quantitated were found to be statistically less in area stained compared to that found in WT mice (Fig. 6C). The expression of mRNA encoding the angiogenic factor VEGF was also decreased in *Bgn*-deficient compared to WT callus at 7 days post-fracture (Fig. S3).

2.5. Bgn binding to VEGF and its effect on VEGF signaling

Because Bgn is found at sites of new bone formation, especially in regions where vessels are forming, coupled with the fact that *Bgn*-deficient mice appear to have less vascularization, suggested that there was a relationship between that Bgn and VEGF. To examine this possibility we first determined whether Bgn could directly bind to VEGF. In this approach, we used a recombinant form of Bgn with a His-tag attached to it and measured its ability to bind to recombinant VEGF attached to a solid support system (Fig. 7A). This experiment showed a specific and statistically significant dose-dependent binding of His-tagged human BGN to VEGF. When human BGN core protein (devoid of attached GAG chains) was instead used in the same solid phase binding assay, it also bound to VEGF in a dose dependent manner (Fig. 7B), indicating that the core protein interacts with VEGF. In this latter experiment we found much more non-specific binding in the controls (where no VEGF was bound to the plate). For this reason we decreased the amount of BGN used from 1.0 μg/ml to 0.25 μg/ml and additionally increased the stringency of the binding and washing and we suspect this is the reason that more VEGF was needed to detect signifi-cant binding to the BGN core protein. We next examined the direct effects of BGN on VEGF induced signaling in human umbilical vein endothelial cells (HUVECs) *in vitro*. Neither the BGN core protein nor the proteoglycan form of BGN enhanced VEGF-induced VEGFR2 phosphorylation (Fig. 7C, top panel) or ERK1/2 phosphorylation (Fig. 7C, third panel). In summary, while BGN could bind to VEGF, its function in regulating down-stream signaling seems to be indirect and, rather, potentially related to VEGF storage or stability.

3. Discussion

3.1. Bgn, osteogenesis and tissue repair

The importance of Bgn in fracture healing has been suspected from several lines of evidence. First, Bgn deficient bones have lower mass and are more fragile based on biomechanical evaluation of the forces needed to bend and break them compared to WT bones (Xu et al., 1998). Subsequent work using Bgn-deficient mice subject to marrow ablation showed that they had delayed bone formation during the repair process judged by μCT analysis of diaphysis of the bone (Chen et al., 2003). Several reports have confirmed the paradigm that Bgn has important roles in modulating cytokines and growth factors in ways that ultimately affect osteoprogenitor/stem cell fate. Adherent cells isolated from the bone marrow (bone marrow stromal cells, or BMSCs) are capable of differentiating into multiple cell types including osteoblasts, marrow stromal cells, adipocytes and chondrocytes. Using BMSCs isolated from *Bgn*-deficient mice Chen et al. (2002) showed that they responded poorly to TGF-beta (TGF-β) ultimately affecting their relative clonogenic capacity (colony forming efficiency or CFUf) and their ability to produce type I collagen. In further work using more homogeneous populations of BMSCs isolated from calvarial bones, Chen et al. (2004) showed that the levels of osteogenic differentiation *in vitro* were reduced in Bgn-deficient cells and that this reduction appeared to be caused by diminished BMP2 binding and subsequent signaling. More recently, the hypothesis that Bgn could modulate Wnts, inducers known to have key roles in bone function, was tested. Using a series of *in vitro* and *in vivo* approaches, Berendsen et al. (2011) showed that the core protein of Bgn could enhance Wnt signaling leading to increased osteogenesis. Pre-clinical work from the Fallon lab showed that intraperitoneal (IP) application of Bgn into a mouse model of muscular dystrophy repaired many of the phenotypes associated with the disease, including synapse receptor expression and even neuromuscular junction (NMJ) function (Amenta et al., 2011, 2012; Young and Fallon, 2012). In light of the fact that Bgn can accumulate and repair tissues that are distant from the site of application (IP) it is reasonable to imagine that treatment with Bgn could be used in some fashion to aid in the bone healing process.

3.2. Biglycan and collagen: relationship to bone structure and function

The overall importance of collagen to bone strength is well known based on knowledge from patients with the inherited disease, Osteo-genesis Imperfecta (OI). Afflicted individuals acquire connective tissue disorders resulting mainly from mutations in type I collagen genes (*COL1A1* and *COL1A2*). Though OI patients have brittle bones that are prone to fracture, most OI patients heal fractures normally, with some reports of delayed hypertrophic callus formation. Using the *oim*/*oim* mouse model for OI (which is null for c*ol1a2*), Delos et al. (2008) found no significant differences in between *oim*/*oim* and WT in callus size or mineralization, as well as no differences in fractured and contra-lateral intact bones. However, using the Brtl/+ mouse model for OI (which is a “knockin” of Col1a1 Gly 349 to Cys), Meganck et al. (2013) found decreased callus stiffness as well as decreased energy to failure, angular displacement to failure and ultimate torque at failure in the Brtl/+ mice compared to WT. More interestingly, they found that 5 weeks post-fracture the Brtl/+ fractured bones had a significant increase in energy to failure compared to intact

contralateral bones, suggesting the callus they produced is actually stronger than their intact bone. The authors explained this phenomenon by the woven nature of the callus bone, which compared to lamellar bone has less parallel orientation of the collagen fibers and concluded that the magnitude of this change in collagen orientation was far greater than the more subtle difference resulting from genotypic alterations. It is interesting to note that segmental defects treated with a collagen carrier alone showed no significant bone formation or bridging (Barnes et al., 1999). In the course of this study, and in previous work from our lab, we found that Bgn deficiency leads to a decrease in Col1a1 mRNA and protein expression (Chen et al., 2002). Electron microscopy studies further showed that skeletal tissues in Bgn-deficient mice have abnormally shaped collagen fibrils (for review see: (Ameye and Young, 2002)). Taken together, it suggests that *Bgn* deficiency may represent a “phenocopy” of ultra bone structure found in certain forms of Osteogenesis Imperfecta (OI) which, like the *Bgn*-deficient mice, have abnormal collagen fibril size and shape (Corsi et al., 2002). It is interesting to speculate that the combined application of collagen with agents such as Bgn, which is known to regulate collagen fibril structure and strength, could be used to improve bone structure and function during healing.

3.3. Proteoglycans and fracture healing

Proteoglycans, whether secreted or membrane-bound, can modify downstream signals by altering the bioavailability and presentation of numerous ligands to the respective receptors. TGF-β activity has long been known to influence bone matrix quality. Furthermore, low bioavailability or expression of TGF-β is associated with an increase in type II collagen expression, thus influencing chondrogenesis and endochondral bone formation. In addition, TGF-β inhibition results in increased mineral to matrix ratio of bone (Nyman and Makowski, 2012). Bone defects treated with TGF-β2 [even a single injection into the callus 4 days after fracture] caused an increase in total callus volume and retardation in callus resorption (Critchlow et al., 1995). FGF (1 and 2) have high affinity to heparin-like glycosaminoglycans abundantly found in the ECM of bones. A single injection of FGF into the fracture gap during the early stages of healing leads to changes in callus size and strength. FGF1 treatment results in increased callus size and weakening of callus strength, whereas FGF2 treatment results in increase callus size and increased mechanical strength (Jingushi et al., 1990; Nakamura et al., 1998). Taken together it is not unreasonable to assume that altering proteoglycan content and therefore their ability to bind and present FGF will result in changes to callus size. Whether small proteoglycans such as Bgn could also modify FGF activity is not clear and needs further investigation.

3.4. Early stages of fracture healing: potential relationship of immunology to Bgn function

As mentioned earlier, fracture healing involves several distinct yet overlapping phases, including acute inflammation, repair, and remodeling that eventually result in restored bone structure. The TGF-β super-family consists of 3 isoforms of TGF-β (1,2,3), BMPs, and other growth and differentiation factors many of which are clearly involved in bone formation and fracture healing. TGF-βs can display pro- and anti-inflammatory activity depending on their context, and are critical to wound healing, immune responses, and fracture healing. Mice deficient in Smad3, a signaling molecule in the TGF-β pathway, have more rapid fracture repair with less cartilage formation in the callus, accompanied by increased osteogenesis and

reduced chondrogenesis (Kawakatsu et al., 2011). Bmp2 has long been known to participate in the signaling pathway that regulates fracture healing. Although shown not to be required for bone formation, *Bmp2*-deficient mice have spontaneous non-healing fractures, and the healing defect appears to be the result of a blockade in the early healing steps, suggesting that Bmp2 is required for initiation of fracture healing (Tsuji et al., 2006). The relationship of small proteoglycans such as Bgn in regulating members of the TGF-β superfamily, including Bmp2, has previously been shown using unchallenged bone tissue (Chen et al., 2002, 2004). It will be important to now determine whether Bgn could have regulatory roles in the early steps of inflammation after fracture/trauma, similar to the ones that have been described in detail above. In this regard, it is interesting to note that fracture healing can be affected by multiple inflammatory conditions including diabetes, autoimmune diseases (Rheumatoid arthritis/RA, lupus) and sepsis. Previous work from Schaefer et al. (Schaefer et al., 2005) showed that Bgn was a critical mediator of the sepsis response using a mechanism that relies on functional toll-like receptors, Tlr2 and Tlr4. It is tempting to speculate that Bgn could also play a regulatory role in the complex immune responses that are now known to unfold during the first phases of bone fracture and repair.

3.5. Concluding remarks and unanswered questions remaining

Several key findings emerged from our study of WT and *Bgn*-deficient mice during fracture healing. First, Bgn expression was found to be very high in the healing bone, coincident with invading blood vessels that are known to be essential to the fracture healing process. μCT and X-ray analysis suggested that the size of the callus formed in Bgn-deficient mice was smaller than WT mice, an observation verified by further histology. At 14 days post-fracture, the forming callus had less cartilage and bone judged by its appearance with H&E staining and by immunohistochemistry for aggrecan and type I collagen, as well as by picrosirius red staining respectively. These analyses indicated that the levels of vessel formation in the *Bgn*-deficient mice were lower than those observed in WT mice. Our work also showed that Bgn could directly bind to VEGF but when its affect on VEGF signaling was tested in HUVECs in vitro neither Bgn core protein nor proteoglycan could further modulate downstream targets of VEGF including phosphorylation of the VEGF receptor and ERK1/2. This leads us to conclude that Bgn's role could be indirect, being one of a “matrix storage” agent, possibly leading to increased stabilization of VEGF in the matrix microenvironment within the callus. In this context it must be noted that BGN is found in endothelial cells (Obika et al., 2013) and it is possible that further addition of BGN to such cells will be ineffective. We can also not exclude the further possibility that in the absence of Bgn, Dcn which goes up, could be inhibitory to vessel ingrowth. Indeed recent work shows that Dcn inhibits endothelial expansion by inducing autophagy (Buraschi et al., 2013). On the other hand, despite their clear structural similarities, Bgn and Dcn have been shown to function differently. For example, in our hands Bgn enhances Lrp6 dependent signaling while Dcn does not. The essential role of vascularization in bone cell signaling and function is well documented (Clarkin and Gerstenfeld, 2013), and the fact that Bgn could play a modulatory role is an important new finding. We do not know at this time what region of the Bgn core protein participates in VEGF binding and function, however, in this regard it is interesting to note that Bgn applied *in vivo* using retrovirus therapy to smooth muscle cells shows clear differences in its response depending on whether GAG chains were

attached (Hwang et al., 2008). Many biological questions remain to be answered including: 1) What structural component of Bgn is involved in fracture healing? 2) Does the delayed and deficient healing in the Bgn-deficient mice lead to weaker bones after repair? 3) Could Bgn be used therapeutically to enhance fracture healing either applied by tissue engineering or systemically? 4) Are the early phases of fracture healing affected by Bgn and if so how does that influence the sequence of repair? 5) Are there yet other unidenti-fied partners that work with Bgn to control skeletal function? It will be interesting to tackle these questions one by one to fully understand the role of Bgn in regulating fracture healing.

4. Materials and methods

4.1. Creating and monitoring fracture healing

The fracture-healing model is shown pictorially in Fig. 1 and was carried out as follows. Male WT or Bgn-KO mice that were six weeks of age (Xu et al., 1998) were anesthetized with isoflurane (2–5% in O_2) (Fig. 1A). Fur was removed from the joint area of the right hind leg with an electric shaver (Fig. 1B). A 5 mm incision was made over the knee joint and the patella tendon exposed as a landmark (Fig. 1D). A 25-gauge (25G) hypodermic needle was inserted into the intracondylar notch of the femur (located directly under the tendon) and subsequently removed. This was done to create a cavity for the insertion of a 23G spinal needle that served to stabilize the bone after fracture. (Fig. 1E). The protruding end of the spinal needle was clipped (Fig. 1F) so that it did not extrude from the surface of the skin. A custom device was then used to fracture the femur (Fig. 1G and H) by placing the mouse in a dorsal position and then inserting the right leg in between the fracture blade and platform. A 200-g weight was then dropped to apply a precise force that generated a single oblique fracture in the femur. An X-ray was immediately taken with continued sedation using a Lumina-XR apparatus (Fig. 1I). Mice having suitable fractures were used for further study. After X-ray analysis, the skin incision was closed with tissue glue (VetBond™). In some experiments pliers were used to create fractures that were evaluated and processed in the same way. Experimental animals were evaluated 7, 14, 21 and 28 days post-fracture by X-ray, μCT, histology, and for mRNA expression as described in greater detail below. Two separate fracture experiments were performed: the first set used 12 WT and 16 *Bgn*-deficient mice and the second used 10 WT and 9 *Bgn*-deficient mice. All procedures with mice were carried out with approval from the Animal Care and Use Committee, NIDCR (#13-676).

4.2. Micro-computed tomography (μCT)

Fractured femurs were harvested 7 and 14 days after the surgery and fixed for 48 h with Z-fix (Cat# 170; Anatech LTD, MI, USA). After transfer to 70% ethanol the bones were scanned and reconstructed with 8-μm isotropic voxels on a μCT analysis system (eXplore Locus SP; GE Healthcare). Reconstructed 3D images were analyzed using eX-plore MicroView (GE Healthcare Life Science). First, the angle of femurs was adjusted to make the fracture plane become parallel to the axial plane. Then a slice image at the fracture line was captured and the cross sectional area (CSA) was measured using ImageJ.

4.3. Histology and tissue staining

For immunohistochemistry, rehydrated sections were enzymatically treated with ABCase (chondroitin sulfate ABC Lyase) and incubated with primary antibodies at 4 °C overnight, including polyclonal rabbit anti-mouse Bgn (1:500 dilution, LF-106; Dr. Larry Fisher, NIH), polyclonal rabbit anti-human type I collagen (1:500 dilution, rabbit antiserum, LF-68; Dr. Larry Fisher, NIH), polyclonal anti-mouse Dcn, (1:500 dilution, LF-114; Dr. Larry Fisher, NIH) (Fisher et al., 1995), polyclonal rabbit anti-mouse aggrecan (1:100 dilution, AB1031; Chemicon), The broad-spectrum immunoperoxidase AEC kit (Picture Plus; Zymed) was subsequently used to detect the immunoactivity according to the manufacturer's instructions. Blood vessel invasion in the fracture area was identified by staining with a horseradish peroxidase (HRP)-conjugated lectin from Bandeiraea simplicifolia (L5391; Sigma-Aldrich, St. Louis, MO). This lectin shows a specific affinity for endothelial cell proteoglycans, as previously described (Mattsson et al., 2002; de Castro et al., 2010). Briefly, sections were incubated with 3% H_2O_2 in PBS for 15 min to inactivate endogenous peroxidase, and non-specific lectin hybridization was blocked with 1% BSA in PBS for 10 min at room temperature. Then, samples were incubated with 50 μg/ml of HRP-lectin in blocking solution for 72 h at 4 °C. After rinsing with PBS, aminoethyl carbazole (AEC) (001122; Life Tech) was used as a chromogen and samples were counterstained with hematoxylin. Lectin stained samples were scanned using Aperio Imagescope slide scanner and 4 captures per sample of 1660 × 930 μm^2 (100×) of the hypertrophic cartilage calcification areas at the fracture site were acquired. Using ImageJ, red staining areas were measured and compared between WT and *Bgn*-KO. Picrosirius red staining for collagen fiber was done using the Picrosirius Red Stain Kit (24901–250; Polyscience, Inc.) and tissue was observed under the polarized light.

4.4. Real time RT-PCR

The callus region of the fractured WT and Bgn-KO femurs ($n = 4$ for each genotype) was dissected out at 7 days post-fracture and immediately submerged in liquid N_2. Total RNA was isolated from the callus using Trizol (Invitrogen). Samples were treated with an RNase-free DNase removal reagent (18068–015; Invitrogen). cDNA was obtained by reverse transcribing total RNA with iScript™ cDNA Synthesis Kit (170–8891; Bio-Rad). Primers were designed using Beacon Designer Software (Bio-Rad) and included the following: *S29* forward 5′ ggagtcacccacggaagttcg 3′, reverse 5′ ggaagcagctggcggcacatg 3′, biglycan (Bgn) forward 5′ acctgtccccttccatctct 3′, reverse 5′ ccgtgtgtgtgtgtgtgtgt 3′, aggrecan (*Acan*) forward 5′ cccggtaccctacagagaca 3′, reverse 5′ acagtgaccctggaacttgg 3′, alkaline phosphatase (*Alp*) forward 5′ gctctccctaccgaccctgttc 3′, reverse 5′ tgctggaagttgcctggacctc 3′ and vascular endothelial growth factor (*Vegf*) forward 5′ ggagaggagcccgccaagg 3′, reverse 5′ agcagtaaagccagggtccagtg 3′. Real-time PCR was performed using primers, iQ™ SYBR® Green Supermix (170–8886; Bio-Rad), and a CFX96™ Real-Time PCR Detection System (Bio-Rad). Each cDNA (5–10 ng) was amplified with an initial denaturation at 95 °C for 10 min, then 95 °C for 15 s and 65 °C for 30 s, for 40 cycles. Gene expression was normalized to the housekeeping gene S29. Melt-curve analysis was routinely run, and the PCR reactions were also analyzed by gel electrophoresis to confirm that a single product of the expected size was amplified.

4.5. Solid phase binding of VEGF to Bgn and VEGF signaling

Ninety-six-well polystyrene plates were coated with recombinant VEGF protein (CYT-336; Prospec, Israel) or BSA in a coating buffer (50 mM $NaHCO_3$–Na_2CO_3 buffer (pH9.6)) overnight at 4 °C. Unbound protein was removed and each well was blocked with 2% BSA in wash buffer. After a 2-h incubation at 37 °C, His-tagged human recombinant Bgn made in HEK 293 cells (see ab151798; abcam®, Cambridge, UK for greater details) diluted with blocking buffer was added and incubated 2 h at 37 °C. In this first binding experiment a concentration of 1 μg/ml of the His-tagged BGN was used based on our previous experience using similar His-tagged proteins. To detect the binding of the two proteins to each other, HRP conjugated anti-His antibody (ab1187; abcam®, Cambridge, UK) diluted with blocking buffer was added and incubated for 2 h at room temperature. After each incubation, the wells were washed 3 times with 200 μl of wash buffer (50 mM Tris– HCl (pH7.4), 150 mM NaCl, 0.05% Tween® 20). The amount of relative binding was visualized using TMB Microwell Peroxidase Substrate System (50-76-11; KLP, MD, USA) and the reaction was stopped with 2 N H_2SO_4. Then absorbance was measured at 450 nm. To determine the specificity of binding between VEGF and Bgn-core protein, 0.1% BSA-PBS was substituted for BGN to coat VEGF. In this case the Bgn core was used that was prepared as described previously (Mercado et al., 2006). In this second experiment we found that 1 μg/ml of biglycan resulted in detectable non-specific color reaction judged by the color detection using all of the same components of the reaction without VEGF added to the system. For that reason we carried out a titration experiment and found that 0.25 μg/ml was optimal and subsequently used in the experiment. To detect the binding between VEGF and BGN in this second experiment, an antibody against human Bgn (LF-112) and HRP conjugated anti-IgG antibody was used.

To examine the effects of Bgn on VEGF signaling, HUVECs were plated into a 6-well plate (1×10^5/well) and cultured for 2 days, followed by a 10 min treatment with 25 or 100 ng/ml recombinant human VEGF (293-VE-CF; R&D Systems) with or without 1 μM recombinant human BGN proteoglycan or core protein (Mercado et al., 2006). Cells were lysed on ice in PhosphoSafe Extraction Reagent (Novagen) supplemented with 1 μg/ml protease inhibitor cocktail (Roche) and protein extracts were cleared by centrifugation at 12,000 rpm for 20 min at 4 °C. Equal amounts of lysates were loaded and separated by SDS-polyacrylamide gel electrophoresis using 4–12% Bis-Tris precast polyacrylamide gels (NuPage; Invitrogen) and MOPS running buffer (Invitrogen), followed by transfer of proteins onto nitrocellulose membranes (Bio-Rad). Blots were blocked with 5% Blotting Grade Blocker Non-Fat Dry Milk (Bio-Rad) in TBS/0.1% Tween 20 (Sigma) before overnight probing at 4 °C with antibodies to the following proteins: Phospho-VEGF Receptor 2 (Tyr1175) (dilution 1:1000; 2478; Cell Signaling Technology), VEGF Receptor 2 (dilution 1:1000; 2479; Cell Signaling Technology), Phospho-p44/42 MAPK (Erk1/2) (Thr202/ Tyr204) (dilution1:2000; 4370; Cell Signaling Technology), p44/42 MAPK (Erk1/2) (dilution 1:1000; 9102; Cell Signaling Technology). Protein bands were visualized using HRP-labeled secondary antibodies (dilution 1:5000; Thermo Scientific), SuperSignal® West Dura Extended Duration Substrate (Pierce Biotechnology) and exposure of the membrane to autoradiography film (Denville Scientific Inc).

4.6. Statistics

To evaluate meaningful differences between controls and experiment samples an unpaired two-tailed Student's *t*-test was used to evaluate the data with the aid of PRISM software and a p value of <0.05 was considered significantly different from control. For real-time RT-PCR values represent mean relative expression ± standard deviation (SD).

Supplementary data to this article can be found online at http://dx. doi.org/10.1016/j.matbio.2013.12.004.

Supplementary Material

Refer to Web version on PubMed Central for supplementary material.

Acknowledgments

We would like to thank Dr. Louis Gerstenfeld and Dr. David Kohn for advice on experimental methodologies and analyses. This research was supported by the Intramural Research Program of the NIH, NIDCR.

Abbreviations

SLRPs	small leucine-rich proteoglycans
Bgn	biglycan
dcn	decorin
VEGF	vascular endothelial growth factor A
BMP	bone morphogenic protein

References

Amenta AR, Yilmaz A, Bogdanovich S, McKechnie BA, Abedi M, Khurana TS, Fallon JR. Biglycan recruits utrophin to the sarcolemma and counters dystrophic pathology in mdx mice. Proc. Natl. Acad. Sci. U. S. A. 2011; 108:762–767. [PubMed: 21187385]

Amenta AR, Creely HE, Mercado ML, Hagiwara H, McKechnie BA, Lechner BE, Rossi SG, Wang Q, Owens RT, Marrero E, Mei L, Hoch W, Young MF, McQuillan DJ, Rotundo RL, Fallon JR. Biglycan is an extracellular MuSK binding protein important for synapse stability. J. Neurosci. 2012; 32:2324–2334. [PubMed: 22396407]

Ameye L, Young MF. Mice deficient in small leucine-rich proteoglycans: novel in vivo models for osteoporosis, osteoarthritis, Ehlers-Danlos syndrome, muscular dystrophy, and corneal diseases. Glycobiology. 2002; 12:107R–116R.

Barnes GL, Kostenuik PJ, Gerstenfeld LC, Einhorn TA. Growth factor regulation of fracture repair. J. Bone Miner. Res. 1999; 14:1805–1815. [PubMed: 10571679]

Berendsen AD, Fisher LW, Kilts TM, Owens RT, Robey PG, Gutkind JS, Young MF. Modulation of canonical Wnt signaling by the extracellular matrix component biglycan. Proc. Natl. Acad. Sci. U. S. A. 2011; 108:17022–17027. [PubMed: 21969569]

Bianco P, Fisher LW, Young MF, Termine JD, Robey PG. Expression and localization of the two small proteoglycans biglycan and decorin in developing human skeletal and non-skeletal tissues. J. Histochem. Cytochem. 1990; 38:1549–1563. [PubMed: 2212616]

Buraschi S, Neill T, Goyal A, Poluzzi C, Smythies J, Owens RT, Schaefer L, Torres A, Iozzo RV. Decorin causes autophagy in endothelial cells via Peg3. Proc. Natl. Acad. Sci. U. S. A. 2013; 110:E2582–E2591. [PubMed: 23798385]

Chen XD, Shi S, Xu T, Robey PG, Young MF. Age-related osteoporosis in biglycan-deficient mice is related to defects in bone marrow stromal cells. J. Bone Miner. Res. 2002; 17:331–340. [PubMed: 11811564]

Chen XD, Allen MR, Bloomfield S, Xu T, Young M. Biglycan-deficient mice have delayed osteogenesis after marrow ablation. Calcif. Tissue Int. 2003; 72:577–582. [PubMed: 12724831]

Chen XD, Fisher LW, Robey PG, Young MF. The small leucine-rich proteoglycan biglycan modulates BMP-4-induced osteoblast differentiation. FASEB J. 2004; 18:948–958. [PubMed: 15173106]

Clarkin CE, Gerstenfeld LC. VEGF and bone cell signalling: an essential vessel for communication? Cell Biochem. Funct. 2013; 31:1–11. [PubMed: 23129289]

Corsi A, Xu T, Chen XD, Boyde A, Liang J, Mankani M, Sommer B, Iozzo RV, Eichstetter I, Robey PG, Bianco P, Young MF. Phenotypic effects of biglycan deficiency are linked to collagen fibril abnormalities, are synergized by decorin deficiency, and mimic Ehlers-Danlos-like changes in bone and other connective tissues. J. Bone Miner. Res. 2002; 17:1180–1189. [PubMed: 12102052]

Critchlow MA, Bland YS, Ashhurst DE. The effect of exogenous transforming growth factor-beta 2 on healing fractures in the rabbit. Bone. 1995; 16:521–527. [PubMed: 7654467]

de Castro LF, Lozano D, Dapia S, Portal-Nunez S, Caeiro JR, Gomez-Barrena E, Esbrit P. Role of the N- and C-terminal fragments of parathyroid-hormone-related protein as putative therapies to improve bone regeneration under high glucocorticoid treatment. Tissue Eng. A. 2010; 16:1157–1168.

Delos D, Yang X, Ricciardi BF, Myers ER, Bostrom MP, Camacho NP. The effects of RANKL inhibition on fracture healing and bone strength in a mouse model of osteogenesis imperfecta. J. Orthop. Res. 2008; 26:153–164. [PubMed: 17729310]

Einhorn TA. The cell and molecular biology of fracture healing. Clin. Orthop. Relat. Res. 1998:S7–S21. [PubMed: 9917622]

Fisher LW, Termine JD, Dejter SW Jr. Whitson SW, Yanagishita M, Kimura JH, Hascall VC, Kleinman HK, Hassell JR, Nilsson B. Proteoglycans of developing bone. J. Biol. Chem. 1983; 258:6588–6594. [PubMed: 6189828]

Fisher LW, Stubbs JT III, Young MF. Antisera and cDNA probes to human and certain animal model bone matrix noncollagenous proteins. Acta Orthop. Scand. Suppl. 1995; 266:61–65. [PubMed: 8553864]

Hwang JY, Johnson PY, Braun KR, Hinek A, Fischer JW, O'Brien KD, Starcher B, Clowes AW, Merrilees MJ, Wight TN. Retrovirally mediated overexpression of glycosaminoglycan-deficient biglycan in arterial smooth muscle cells induces tropoelastin synthesis and elastic fiber formation in vitro and in neointimae after vascular injury. Am. J. Pathol. 2008; 173:1919–1928. [PubMed: 18988796]

Iozzo, RV.; Goldoni, S.; Berendsen, AD.; Young, MF. Small leucine-rich proteogly-cans.. In: Mecham, R., editor. The Extracellular Matrix: An Overview. Springer; Berlin Keldelberg: 2011.

Jingushi S, Heydemann A, Kana SK, Macey LR, Bolander ME. Acidic fibroblast growth factor (aFGF) injection stimulates cartilage enlargement and inhibits cartilage gene expression in rat fracture healing. J. Orthop. Res. 1990; 8:364–371. [PubMed: 2324855]

Kawakatsu M, Kanno S, Gui T, Gai Z, Itoh S, Tanishima H, Oikawa K, Muragaki Y. Loss of Smad3 gives rise to poor soft callus formation and accelerates early fracture healing. Exp. Mol. Pathol. 2011; 90:107–115. [PubMed: 21035443]

Manigrasso MB, O'Connor JP. Characterization of a closed femur fracture model in mice. J. Orthop. Trauma. 2004; 18:687–695. [PubMed: 15507822]

Mattsson G, Carlsson PO, Olausson K, Jansson L. Histological markers for endothelial cells in endogenous and transplanted rodent pancreatic islets. Pancreatology. 2002; 2:155–162. [PubMed: 12123096]

Meganck JA, Begun DL, McElderry JD, Swick A, Kozloff KM, Goldstein SA, Morris MD, Marini JC, Caird MS. Fracture healing with alendronate treatment in the Brtl/+ mouse model of osteogenesis imperfecta. Bone. 2013; 56:204–212. [PubMed: 23774443]

Mercado ML, Amenta AR, Hagiwara H, Rafii MS, Lechner BE, Owens RT, McQuillan DJ, Froehner SC, Fallon JR. Biglycan regulates the expression and sarcolemmal localization of dystrobrevin, syntrophin, and nNOS. FASEB J. 2006; 20:1724–1726. [PubMed: 16807372]

Morgan EF, Mason ZD, Chien KB, Pfeiffer AJ, Barnes GL, Einhorn TA, Gerstenfeld LC. Micro-computed tomography assessment of fracture healing: relationships among callus structure, composition, and mechanical function. Bone. 2009; 44:335–344. [PubMed: 19013264]

Nakamura T, Hara Y, Tagawa M, Tamura M, Yuge T, Fukuda H, Nigi H. Recombinant human basic fibroblast growth factor accelerates fracture healing by enhancing callus remodeling in experimental dog tibial fracture. J. Bone Miner. Res. 1998; 13:942–949. [PubMed: 9626625]

Nyman JS, Makowski AJ. The contribution of the extracellular matrix to the fracture resistance of bone. Curr. Osteoporos. Rep. 2012; 10:169–177. [PubMed: 22527725]

Obika M, Vernon RB, Gooden MD, Braun KR, Chan CK, Wight TN. ADAMTS-4 and biglycan are expressed at high levels and co-localize to podosomes during endothelial cell tubulogenesis in vitro. J. Histochem. Cytochem. 2013; 62:34–49. [PubMed: 24051360]

Schaefer L, Babelova A, Kiss E, Hausser HJ, Baliova M, Krzyzankova M, Marsche G, Young MF, Mihalik D, Gotte M, Malle E, Schaefer RM, Grone HJ. The matrix component biglycan is proinflammatory and signals through Toll-like receptors 4 and 2 in macrophages. J. Clin. Invest. 2005; 115:2223–2233. [PubMed: 16025156]

Tsuji K, Bandyopadhyay A, Harfe BD, Cox K, Kakar S, Gerstenfeld L, Einhorn T, Tabin CJ, Rosen V. BMP2 activity, although dispensable for bone formation, is required for the initiation of fracture healing. Nat. Genet. 2006; 38:1424–1429. [PubMed: 17099713]

Xu T, Bianco P, Fisher LW, Longenecker G, Smith E, Goldstein S, Bonadio J, Boskey A, Heegaard AM, Sommer B, Satomura K, Dominguez P, Zhao C, Kulkarni AB, Robey PG, Young MF. Targeted disruption of the biglycan gene leads to an osteoporosis-like phenotype in mice. Nat. Genet. 1998; 20:78–82. [PubMed: 9731537]

Young MF, Fallon JR. Biglycan: a promising new therapeutic for neuromuscular and musculoskeletal diseases. Curr. Opin. Genet. Dev. 2012; 22:398–400. [PubMed: 22841370]

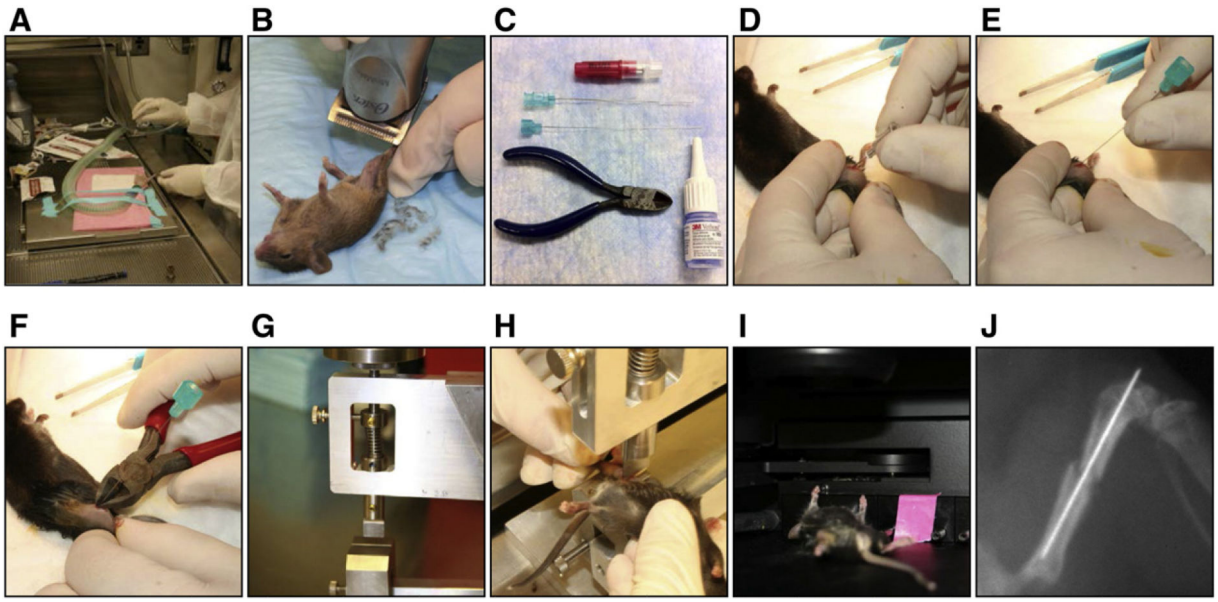

Fig. 1.

Experimental design to create reproducible fractures A: Isoflurane is applied to anesthetize mice. B: Area around the knee is shaved. C: Needles, pliers and glue used to create and stabilize the fracture. D: 23G needle is inserted into the femur to create space for stabilizing needle. E: Catheter needle inserted into the femur prior to fracture. F: Needle clipped to fit the femur. G: Side view of fracture device. H: Positioning the femur for fracture. I: X-ray images were done under anesthesia using the Lumina-XR machine to confirm fracture. J: Typical fracture analyzed. Left leg served as control.

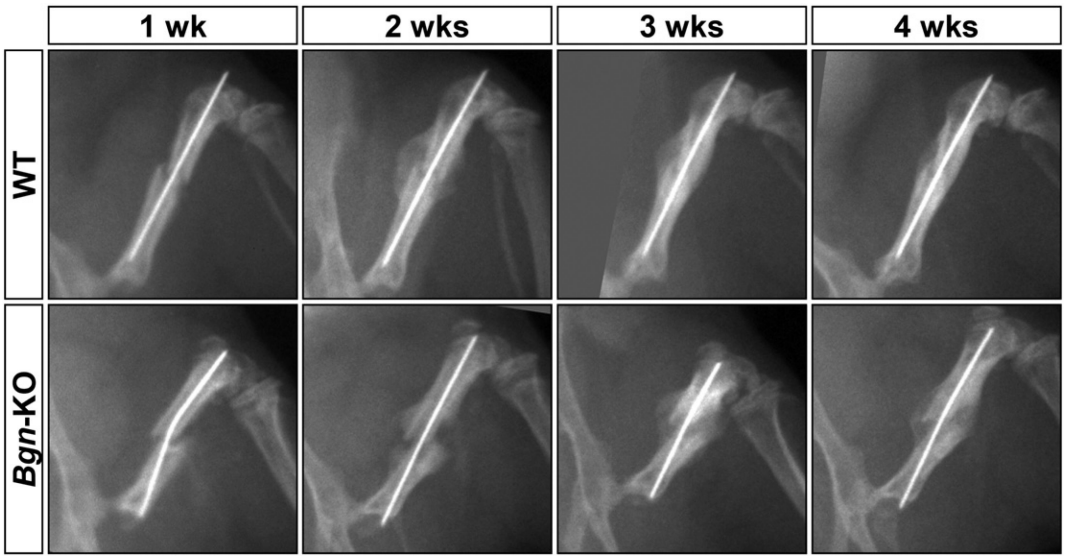

Fig. 2.

X-ray analysis of fractured bone with healing. Femurs from 6-week-old mice were fractured after prior stabilization and the healing process analyzed every week for 4 weeks. *Bgn*-deficient bones fractured more easily and appeared to have delayed healing. Top panels; WT bones, bottom panel; *Bgn*-KO bones.

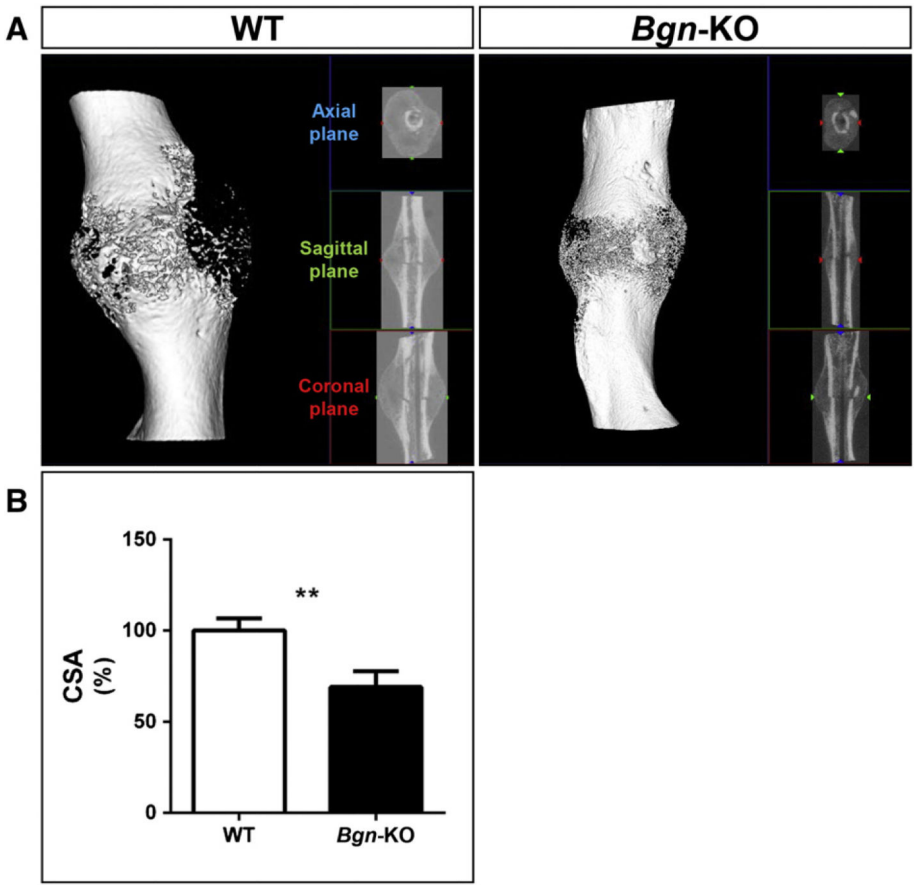

Fig. 3.

μCT analysis of the healing callus. A: Three dimensional rendering of a typical callus area 14 days post-fracture. Left panel; WT femur, right panel; *Bgn*-KO femur. B: The callus area was reconstructed and the cross sectional area (CSA) was measured ($n = 3$ for each genotype). ** $p < 0.01$.

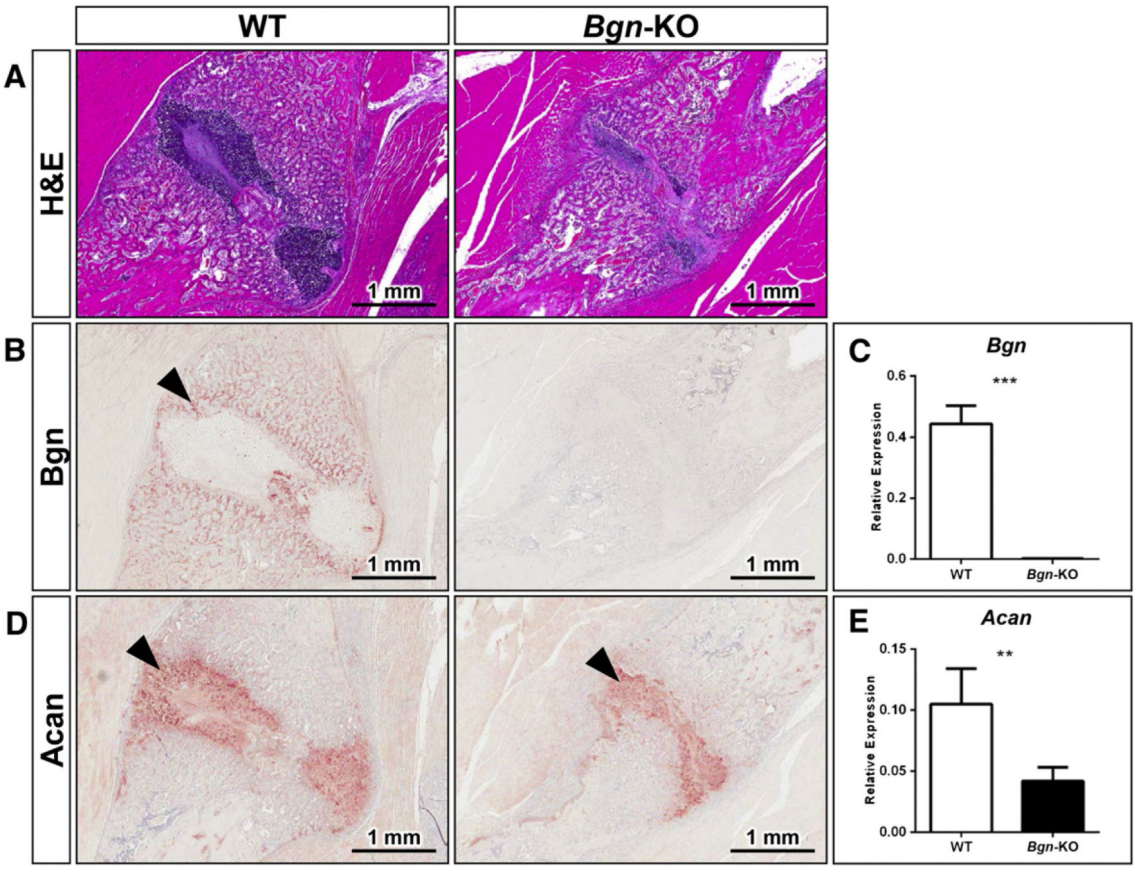

Fig. 4.

Biglycan and aggrecan expression in the healing callus. A: H&E staining of fracture callus area in WT (left) and *Bgn*-KO (right) mice with size bars shown in the lower right corner. B: Immunohistochemistry showing expression of Bgn in the newly formed woven bone 14 days post-fracture (left panel black arrowhead). C: Expression levels of *Bgn* mRNA in the callus 7 days post-fracture relative to S29 mRNA. D: Immunohistochemistry showing aggrecan (Acan) expression 14 days post-fracture. E: Expression levels of *Acan* mRNA in the callus 7 days post-fracture relative to S29 mRNA. *** $p < 0.001$ WT vs. *Bgn*-KO, ** $p < 0.01$ WT vs. *Bgn*-KO.

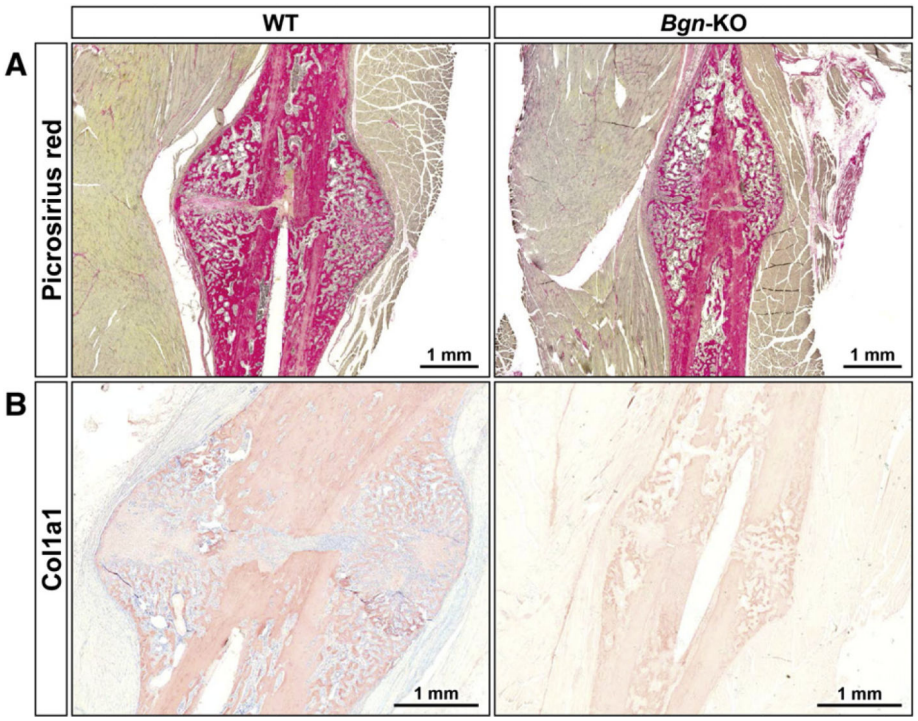

Fig. 5.

Collagen expression in the fracture callus. A: Picrosirius red staining of callus forming around the fractured bones from WT (left) and *Bgn*-KO (right) mice 14 days post-fracture, size bars shown in lower right corner. B: Immunohistochemistry showing relative levels of Col1a1 expression in the bone and in the surrounding callus in bones 14 days post-fracture from WT (left) and *Bgn*-KO (right). Size bars are shown in the lower right corner.

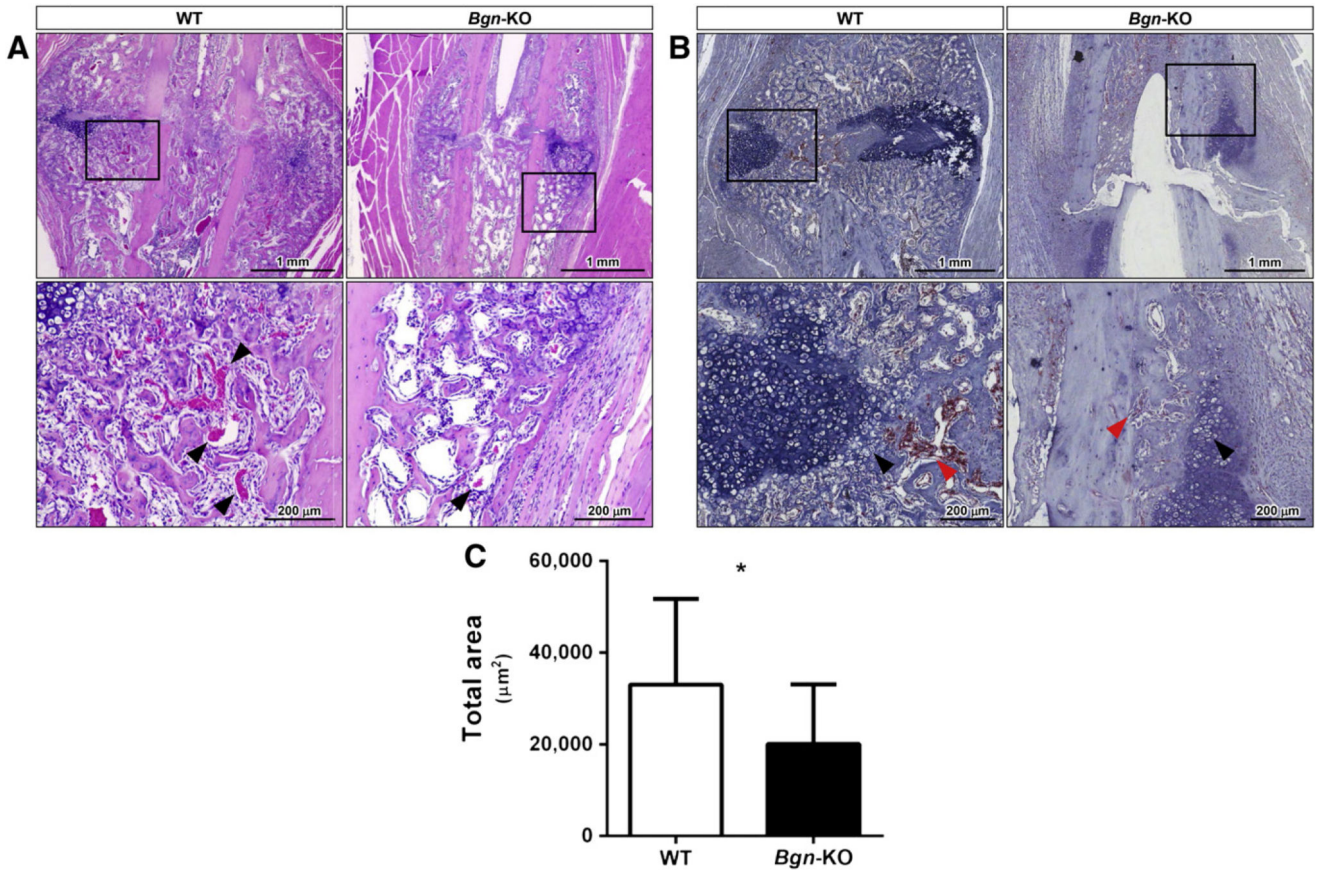

Fig. 6.

Vascular invasion is diminished in the healing callus of *Bgn*-KO mice. A: H&E staining of the healing callus region 14 days post-fracture from WT (left) and Bgn-KO (right). The region in the black box is shown in higher power below with black arrowheads pointing to vessels filled with red blood cells. B: Immunohistochemistry of the callus from WT (left) and *Bgn*-KO (right) fractured bones showing binding of lectin to endothelial cells (red stain). The counterstain with hematoxylin highlights the forming cartilage (dark blue, black arrowheads) relative to the location of the infiltrating vessels (red arrowheads). Size bars are shown in the lower right corner. C: Quantification of the lectin positive area measuring 14 separate areas from $n = 4$ for WT and 10 separate areas from $n = 3$ for Bgn-deficient mice. * $p < 0.05$.

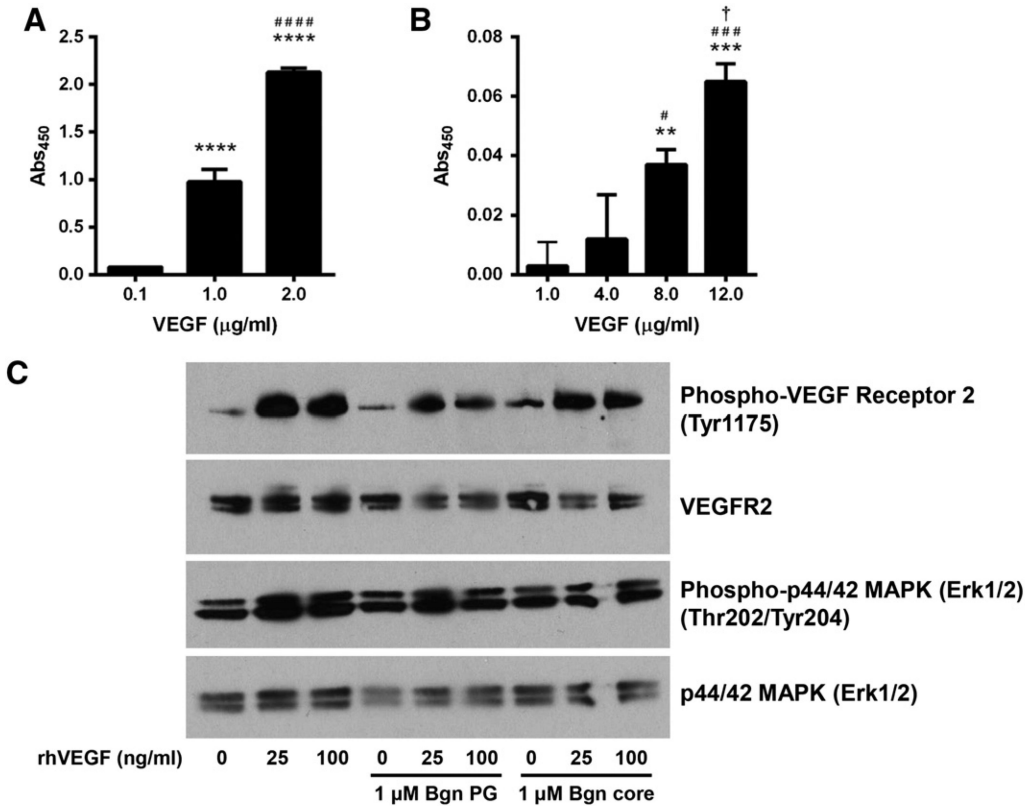

Fig. 7.

Bgn binds to VEGF but does not enhance VEGF-induced signaling. A: The ability of Bgn with a His-tag to bind to increasing doses of VEGF, * compared to 0.1 μg/ml, # compared to 1.0 μ/ml. $n = 5$ for each experimental variable. The absorbance at 450 nm is a measure of BGN concentration (binding). B: The ability of Bgn core protein to bind to increasing doses of VEGF, * compared to 0.1 μg/ml, # compared to 4.0 μg/ml, † compared to 8.0 μg/ml. $n = 3$ for each experimental variable. The absorbance at 450 nm is a measure of BGN concentration (binding). One symbol, $p < 0.05$, two symbols, $p < 0.01$, three symbols, p b 0.001, four symbols, p b 0.0001. C. VEGF induced signaling is not significantly affected by addition of either Bgn PG or Bgn core protein.